

Formation of *n*-type CoSi monosilicide film which can be used in instrumentation

I. R. Bekpulatov*, G. T. Imanova^{†,‡}, T. S. Kamilov*,
B. D. Igamov* and I. Kh. Turapov*

**Tashkent State Technical University,
Tashkent, Uzbekistan*

[†]*Institute of Radiation Problems,
Azerbaijan National Academy of Sciences,
Baku AZ 1143, Azerbaijan*

[‡]*gunel_imanova55@mail.ru*

Received 19 July 2022

Revised 2 August 2022

Accepted 4 October 2022

Published 25 November 2022

There arises the formation of thin films of cobalt monosilicide (CoSi) deposited into the base surface of SiO₂/Si (111) using magnetron ion-plasma sputtering and subsequent thermal annealing. It was found that, in addition to the formation of CoSi silicide, also there are Co and Si atoms that do not form bonds on the surface. Therefore, in this work, we studied the surface morphology and composition of a CoSi silicon target using a scanning electron microscope. The study, silicide CoSi, was chosen as the target and standard SiO₂/Si (111) was used as the substrate. The surface morphology and composition of the CoSi silicon film obtained by scanning electron microscopy had been studied. The paper reports on a method, morphology of the surface of a CoSi silicon film obtained using Raman microscopy. The results obtained are based on the fact that they were obtained using a modern magnetron sputterer, a high-vacuum thermal heater and modern devices.

Keywords: Cobalt monosilicide (CoSi); SiO₂/Si (111); scanning electron microscope; Raman microscopy.

PACS numbers: 71.10.-w, 75.10.Dg, 75.30.Et, 75.50.Lk, 75.50.Ww

1. Introduction

In recent years, an important task is the creation of photovoltaic and thermoelectric materials,¹⁻⁴ the study of their electronic, physical and transport properties.

[‡]Corresponding author.

An analysis of studies carried out in this direction shows that the problem of creating microelectronic converters that provide a power of several microwatts is very relevant.⁵

Cobalt monosilicate (CoSi) is known as a semimetal with good electrical parameters.⁶ To date, data have been obtained on the electronic structure and other parameters of CoSi silicide, as well as many other similar silicides (MnSi, CrSi, FeSi). However, the transport properties of these silicon films have not been studied enough. Therefore, there are certain problems in the practical use of high-performance silicon films. One of the topical issues of our time is not only the study of their transport properties, but also the formation of films of CoSi and other silicides by new modern methods. The Co-Si system is a convenient platform in the technology of creating integrated thermoelectric converters. For example, CoSi monosilicide has been found to have a much higher efficiency than other monosilicide films.^{8,9}

Obtaining an atomically clean surface of silicon and gallium arsenide is an urgent problem of electronic instrumentation, as well as the results of experimental studies and various technological operations carried out to create device elements based on Si and GaAs largely depend on the state of their initial surface.

Crystal surface cleaning is often used by direct and indirect (thermal irradiation, electron bombardment, laser annealing) heating at a temperature below the melting point of the sample. The main disadvantage is that thermal annealing leads to a redistribution of impurities in the bulk of the sample or even to their segregation on the surface, followed by the formation of very strong compounds.^{10,11} Ion sputtering is an effective method of cleaning, which consists in bombarding the surface of crystals with Ar^+ ions with an energy of 0.5–5 keV at grazing angles of $<15^\circ$. The disadvantage of the method is that ion bombardment destroys the surface structure.^{12–14}

The pressure behavior of the competing intra- and inter-chain magnetic interactions was analyzed on the basis of obtained structural data and their role in the formation of the magnetic phase diagram is discussed. The pressure behavior of the Néel temperature of the commensurate AFM phase was evaluated within the mean field theory approach and a good agreement with the experimental value $dTNC/dP = 0.65 \text{ K/GPa}$ was obtained.²⁴

The samples were analyzed using X-ray diffraction (XRD) and energy dispersive spectroscopy (EDS) to study the microstructural and composition changes. The XRD results showed the crystalline structure for the sample before and after irradiation (with gamma irradiation dose 9.7, 48.5 and 97 kGy). Amorphization of the sample began at the gamma irradiation dose of 145.5 kGy. Increase in gamma irradiation dose had an inverse effect on the activation energy and had a directly proportional effect on the lattice volume.^{25,26}

The effects of preliminary radiation-oxidative treatment on the current density and current–voltage characteristic of metallic zirconium have been studied. The

contribution of preliminary radiation-oxidative treatment to the change in the electrophysical characteristics during thermal and radiation-thermal tests in the contact of zirconium with water is revealed.²⁷

The XRD spectrum of the nano-ZrO₂ compound was drawn and the crystal structure was determined at room temperature and under normal conditions. Radiation-thermal decomposition of water on nanosized ZrO₂ in the temperature range of $T = 300\text{--}673$ K has been studied by Fourier transform infrared spectroscopy and Raman spectroscopy.²⁸

It is known from the literature that the formation of CoSi, Co₂Si and CoSi₂ structures is possible in the Co–Si system, and it has been confirmed that various contacts, as well as *n*- and *p*-type films, can be formed from these structures.^{7,15} The formation and use of *n*-type CoSi films with high thermal properties is still considered one of the most important problems. The purpose of this work is to create a technique for obtaining a high-quality *n*-type CoSi film with high thermal properties.

2. Experimental

The experiments were carried out on an EPOS-PVD-DESK-PRO setup designed for deposition of one-sided thin-film coatings by magnetron heating of substrates. It has the following characteristics: (1) vacuum level 10^{-4} Pa; (2) target diameter 76 mm; (3) film deposition rate 3–7 Å/s; (4) the accuracy of measuring the film thickness is 0.1 Å.¹⁶

Silicide CoSi was chosen as the target (Fig. 1), and standard SiO₂/Si (111) was used as the substrate.

Before sputtering the CoSi silicon magnetron, the surface of the SiO₂/Si (111) bases was cleaned in two ways:

- (1) Cleaning the surface of SiO₂/Si (111) silicon wafers ($d = 60$ mm) in an ammonia-peroxide mixture at a temperature of 60–70°C, washing in deionized water, drying in a centrifuge.
- (2) Vacuum treatment (cleaning) of the surface of a group plate with an argon plasma flow on EPOS-PVD-DESK-PRO. The plasma flow is created by a source of ions with a cold cathode at a voltage of 2–3 kV and a current of up to 100 mA in a stream for 3–5 min on a rotating equipment with plates.

When silicon CoSi was deposited in the magnetron, the substrate was heated to $T_{\text{sub}} = 250^\circ\text{C}$ and a thin CoSi silicide film with a thickness of $d = 0.25$ μm was obtained.

Additional heating of the formed thin CoSi silicide film was carried out in a UVN-75R-1 universal semi-automatic vacuum apparatus. A vacuum of 10^{-5} Pa was created in the apparatus. The samples were heated to 600°C for 1 h and slowly cooled.¹⁷

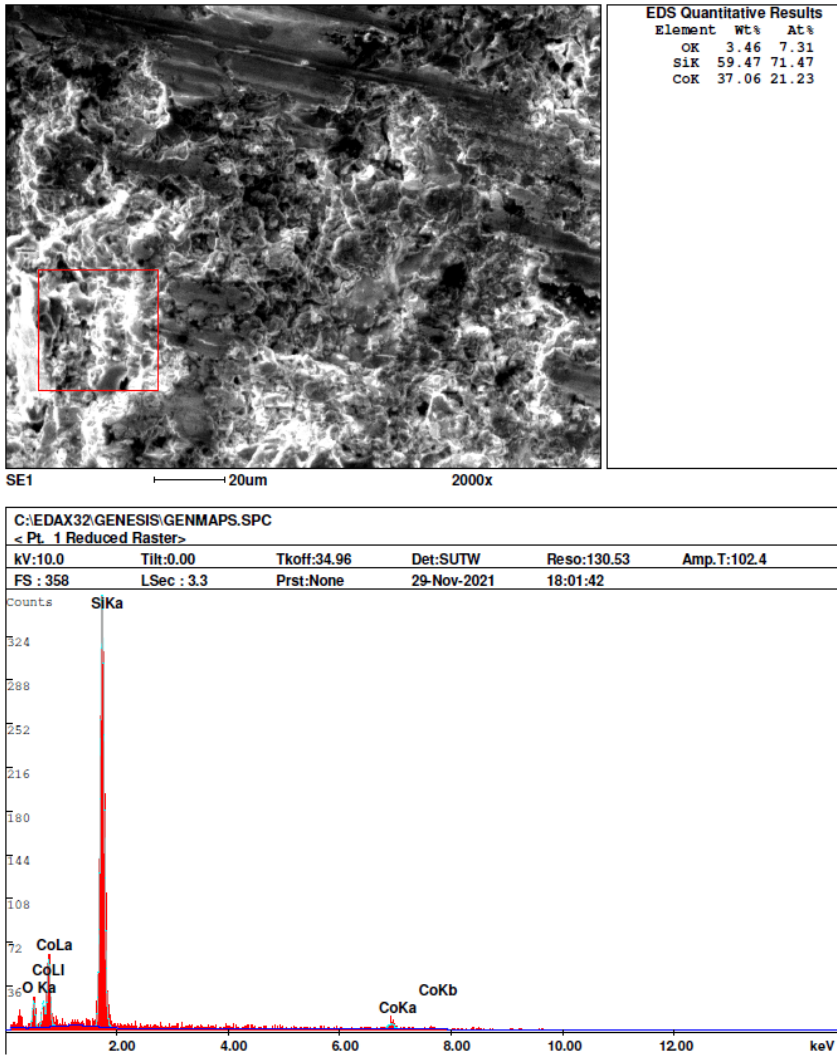


Fig. 1. (Color online) Morphological and composite image of the CoSi target obtained using a scanning electron microscope.

Information about the microstructure, the degree of crystal homogeneity, the size and shape of grains and precipitates, their orientations in the matrix, the presence of pores and cracks are necessary to understand the mechanism of heat and electrical transfer processes in a thermoelectric material. Scanning electron microscopy (SEM) makes it possible to obtain general and local information about the sample microstructure with high accuracy.^{18–20} The resolution of a scanning electron microscope depends on the diameter of the electron beam and on the size of the region of interaction between the electron probe and the sample. Thus, depending on the average atomic number of the substance, by varying the accelerating

Int. J. Mod. Phys. B Downloaded from www.worldscientific.com by GuneI Imanova on 01/08/23. Re-use and distribution is strictly not permitted, except for Open Access articles.

voltage from 30 kV to 1 kV, one can obtain data on the microstructure of the sample from a depth of several microns to hundreds of nanometers. Before placing the target on the magnetron, the composition and structure of the target were examined under a Quanta 200 3D scanning electron microscope (FEI Company).

Using a RENISHAW microscope (in via Raman microscope) with a wavelength of 532 nm (Ne–Cd), the composition of the resulting CoSi thin silicon film and the chemical bonds formed in it were observed.

The electrophysical properties of CoSi silicide films were determined on a modern HMS-3000 instrument.

3. Results and Discussion

Figure 2 shows the morphology and composition of the formed CoSi/SiO₂/Si thin silicon film obtained using a scanning electron microscope.²¹

The surface shown in Fig. 2 shows the morphology of a CoSi silicon film with smooth but known defects. The main reason for the formation of these defects is that, during the deposition of CoSi, various nanosized pieces of CoSi are deposited on the substrate. To minimize these defects and the amount of unbound Co and Si atoms, the film is heated at 600°C for 1 h in high vacuum (10⁻⁶ Pa).

The surface structure of CoSi/SiO₂/Si (111) formed after thermal heating, obtained using a RENISHAW microscope (in via Raman microscope), is shown in Fig. 3. As can be seen from this picture, the surface is not perfectly smooth.

The thin CoSi film with a thickness of $d = 0.25 \mu\text{m}$ caused some problems in observing Raman scattering peaks due to the fact that the oscillation frequencies between the CoSi silicide lattices were very low. Therefore, they had to be investigated in specific frequency intervals. Raman vibration frequencies range from 100 cm⁻¹ to 400 cm⁻¹ in the range 148.242, 175.289, 202.254, 223.381, 246.372, 322.345, 362.386 cm⁻¹. The peaks are Raman scattering peaks belonging to the CoSi monosilicide.

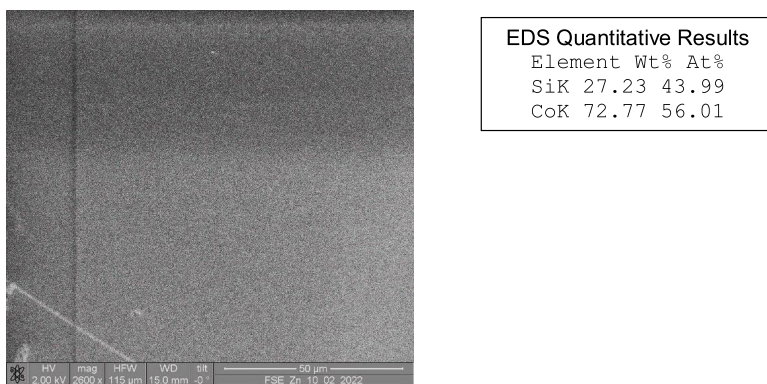


Fig. 2. Surface morphology and composition of the CoSi silicon film obtained by SEM.

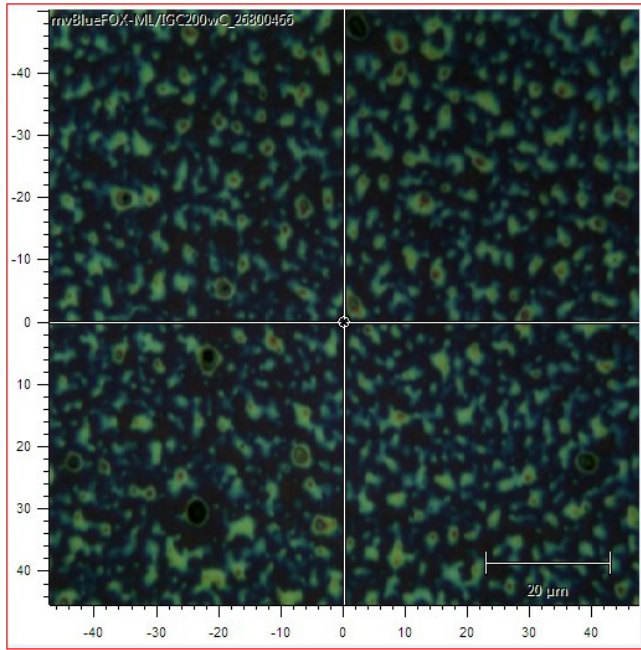


Fig. 3. (Color online) Morphology of the surface of a CoSi silicon film obtained using Raman microscopy.

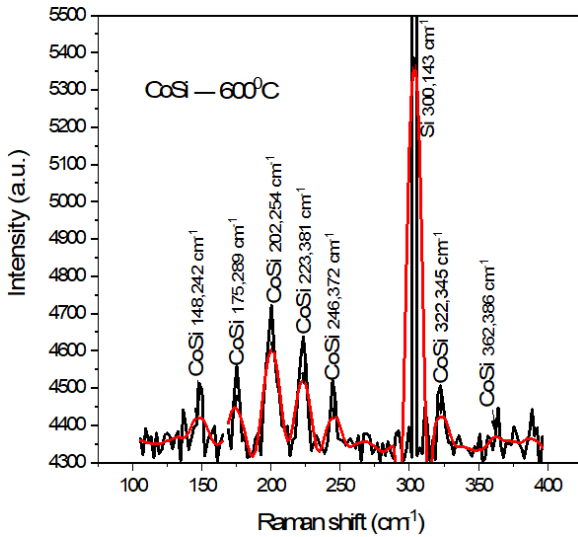


Fig. 4. (Color online) Raman spectra of the CoSi silicon film in the range 100–400 cm^{-1} .

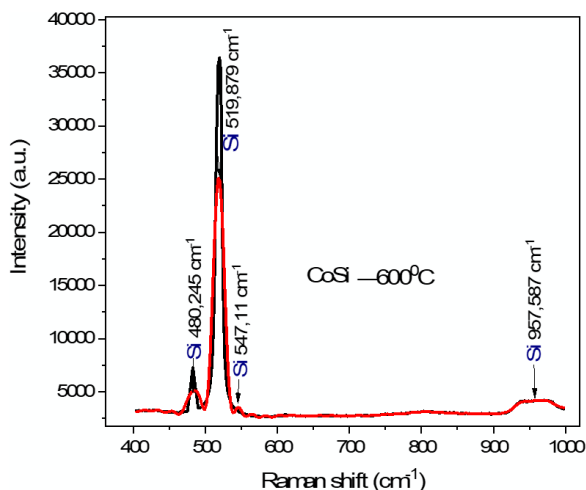


Fig. 5. (Color online) Raman scattering spectra in the range 400–1000 cm^{-1} of a CoSi silicon film.

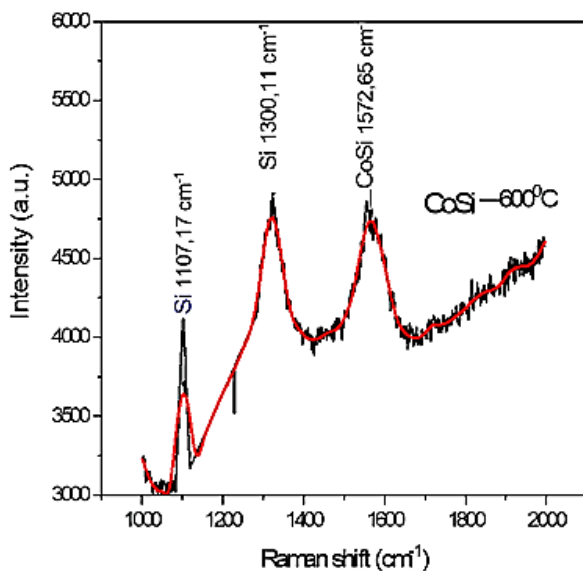


Fig. 6. (Color online) Raman scattering spectra of a CoSi silicon film in the range 1000–2000 cm^{-1} .

The Raman peaks at 480.245, 547.11, 957.587 cm^{-1} , observed in the range 400–1000 cm^{-1} , are Raman peaks belonging to amorphous silicon, the peaks in the region of 519.879 cm^{-1} belong to crystalline silicon, which are Raman peaks. This shows that we can observe Raman peaks belonging to both amorphous silicon and crystalline silicon in the vibration range from 400 cm^{-1} to 1000 cm^{-1} (Fig. 5).

Table 1.

Electrophysical units	Volume concentration	Mobility	Surface resistance	Resistivity	Hall coefficient	Magneto-resistance	Surface concentration	Electrical conductivity
Unit rev.	$1/\text{cm}^3$	$\text{cm}^2/\text{V} \cdot \text{s}$	Ω/cm	$\Omega \cdot \text{cm}$	cm^3/C	Ω	$1/\text{cm}^2$	$1/\Omega \cdot \text{cm}$
CoSi	$1.524 \cdot 10^{20}$	1.217	$1.346 \cdot 10^3$	$9.337 \cdot 10^{-4}$	$-5.228 \cdot 10^{-2}$	$1.295 \cdot 10^{-3}$	$-3.81 \cdot 10^{15}$	$1.071 \cdot 10^3$

Figure 6 shows the Raman peaks of a thin CoSi silicon film in the range 1000–2000 cm^{-1} for 1107.17 cm^{-1} amorphous silicon, 1300.11 cm^{-1} for crystalline silicon. It can be seen from these results that during film formation, as mentioned above, during magnetron sputtering, CoSi and Si atoms are separated from the CoSi target and deposited on the substrate.^{22,23}

Based on the results obtained by the Raman microscope and the results obtained by the scanning electron microscope, it can be seen that the composition of the CoSi target and the composition of the CoSi thin silicon film are almost the same.

An analysis of the results of research on CoSi thin silicon films shows that they can be used in the future as an *n*-type physical material in photovoltaic and thermoelectric devices.

The table lists the electrophysical properties of a thin CoSi film obtained on the basis of studies on a modern HMS-3000 device.

4. Conclusion

In this work, we studied the surface morphology and composition of a CoSi silicon target using a scanning electron microscope. Thin CoSi silicon films were formed from a CoSi target using a modern device for magnetron sputtering EPOS-PVD-DESK-PRO, and the electrophysical properties of the resulting thin CoSi silicon films were studied. The composition of the formed CoSi silicide thin film and the chemical bonds formed in it have been studied, and the electrophysical properties of CoSi silica thin films have been determined. According to the research results, it can be noted that the compositions of CoSi silicide in the target and in a thin film of CoSi silicide are close to each other.

An analysis of the research results shows that a thin film of CoSi silicide can be widely used as a semiconductor element to replace materials with an *n*-type physical character and, in the future, as active parts of modern micro- and nano-electronic devices.

Acknowledgments

We express our gratitude to the head of the laboratory of the Institute of Ion-Plasma and Laser Technologies of the Uzbek Academy of Sciences V. M. Rotshtein, Professor V. V. Klechkovskaya of the Institute of Crystallography. Named of L. V. Shubnikova Federal Research Center “Crystallography and Photonics” RAS, and Professor of the Scientific Laboratory of Microelectronics and Nanoelectronics of the Karshi State University M. T. Normuradov.

References

1. Z. Lu *et al.*, *Nanomaterials* **11**, 2844 (2021), doi:10.3390/nano11112844.
2. S. B. Donaev, A. K. Tashatov and B. E. Umirzakov, *J. Surf. Invest., X-Ray Synchrotron Neutron Tech.* **9**, 406 (2015), doi:10.1134/S1027451015020263.

3. K. Mamadalieva and Y. E. Minamatov, *Middle Eur. Sci. Bull.* **19**, 178 (2021), doi:10.47494/mesb.2021.19.956.
4. G. Imanova and I. Bekpulatov, *Am. J. Nano Res. Appl.* **9**, 32 (2021), doi:10.11648/j.nano.20210904.11.
5. L. K. Mamadalieva and A. G. Tukhtasinov, *Middle Eur. Sci. Bull.* **19**, 365 (2021), doi:10.47494/mesb.2021.19.1000.
6. T. S. Kamilov et al., *Appl. Sol. Energy* **55**, 380 (2019), doi:10.3103/S0003701X19060057.
7. V. S. Kuznetsova et al., *Semiconductors* **53**, 748 (2019).
8. H. J. Goldsmid, *Introduction to Thermoelectricity*, Springer Series in Materials Science, Vol. 121 (Springer, Berlin, 2016), doi:10.1007/978-3-662-49256-7.
9. G. J. Snyder and E. S. Toberer, *Nat. Mater.* **7**, 105 (2008), doi:10.1038/nmat2090.
10. H. Wang et al., *Proc. Natl. Acad. Sci. USA* **109**, 9705 (2012), doi:10.1073/pnas.1111419109.
11. Y. V. Granatkina and Z. M. Dashevsky, *Semiconductors* **56**, 7 (2022).
12. M. I. Fedorov and V. K. Zaitsev, *CRC Handbook of Thermoelectrics*, ed. D. M. Rowe (CRC Press, New York, 1991), p. 321.
13. S. Asanabe, D. Shinoda and Y. Sasaki, *Phys. Rev.* **134**, A774 (1964).
14. D. A. Pshenay-Severin et al., *J. Phys., Condens. Matter* **30**, 135501 (2018).
15. C. K. Nichenametla et al., *J. Inorg. Gen. Chem.* **646**, 1231 (2020), doi:10.1002/zaac.202000084.
16. V. V. Klechkovskaya et al., *Uzbek J. Phys.* **22**, 43 (2021), doi:10.52304/.v23i3.263.
17. L. L. Ilyin, V. V. Plihunov and L. M. Petrov, Functionality of vacuum ion-plasma surface treatment of structural materials Sb, in *Proc. 8th Int. Conf.* (Polytechnic University, St. Petersburg, 2007), pp. 77–80.
18. A. S. Orekhov et al., *Semiconductors* **51**, 925 (2017).
19. A. S. Orekhov et al., *Semiconductors* **51**, 740 (2017).
20. A. S. Orekhov et al., *Russ. Nanotechnol.* **11**, 37 (2016).
21. F. Y. Solomkin et al., *Semiconductors* **53**, 32 (2019), doi:10.11648/j.nano.20210904.11.
22. S. G. Yastrebov et al., *Lett. ZhTF* **30**, 47 (2004).
23. P. Vandenabeele, *Practical Raman Spectroscopy: An Introduction* (Wiley, Chichester, 2013).
24. D. P. Kozlenko et al., *Phys. Rev. B* **98**, 134435 (2018).
25. M. N. Mirzayev et al., *Silicon* **11**, 2499 (2019).
26. M. N. Mirzayev et al., *Mod. Phys. Lett. B* **32**, 1850151 (2018).
27. T. Agayev, G. Imanova and A. Aliyev, *Int. J. Mod. Phys. B* **36**, 2250115 (2022).
28. G. T. Imanova, T. N. Agayev and S. H. Jabarov, *Mod. Phys. Lett. B* **35**, 2150050 (2021).